

Model order reduction for a flow past a wall-mounted cylinder

W. STANKIEWICZ¹), K. KOTECKI¹), M. MORZYŃSKI¹),
R. ROSZAK¹), W. SZELIGA²)

¹) *Division of Virtual Engineering
Institute of Combustion Engines and Transport
Poznan University of Technology
Piotrowo 3
60-965 Poznań, Poland
e-mail: witold.stankiewicz@put.poznan.pl*

²) *Faculty of Machines and Transportation
Poznan University of Technology
Piotrowo 3
60-965 Poznań, Poland*

REDUCED ORDER MODELS allow quickly predict fluid behaviour and to better understand flow phenomena. They are the key enablers of closed-loop flow control. In this paper, reduced-order model (ROM) of an incompressible flow around a wall-mounted cylinder is constructed, by means of Galerkin projection of Navier–Stokes equations onto space spanned by the most dominant eigenmodes of dynamic mode decomposition (DMD). Additionally, genetic algorithm-based calibration is applied to improve the predictive performance of the model. The resulting low-dimensional model of the flow consists of six degrees of freedom and precisely reproduces the dynamics of limit cycle oscillations.

Key words: ROM, Galerkin projection, DMD, CFD.

Copyright © 2016 by IPPT PAN

1. Introduction

NUMERICAL SIMULATIONS OF FLUID FLOW, based on the direct numerical simulation (DNS) of Navier–Stokes equations, provide fundamental knowledge about flow phenomena that occur at low-Reynolds numbers and that persist at high-Reynolds number regimes [1].

However, this approach, as well as even simpler models like large eddy simulation (LES), detached eddy simulation (DES) or even Reynolds-averaged Navier–Stokes (RANS), are too time-consuming to be used in real-time, feedback control of fluid flow.

All of these “high-fidelity” models require computational grids of the order of thousands (2D) or millions (3D) of degrees of freedom to cover all important vertex scales and capture the flow physics.

Consequently, they are very time-consuming – especially when complex geometries are analyzed.

More importantly, the models with a large number of degrees of freedom are not robust – to provide for real-time feedback flow control, the number of inputs and outputs of the controller have to be as small as possible.

The problems of being too time consuming and not being robust enough can be solved by using low-fidelity, reduced order models (ROMs) instead of the models mentioned above. These robust models, consisting of a few equations, are key enablers of feedback flow control [2]–[5]. A review of techniques for nonlinear model-based flow control can be found in [6].

In this paper, model order reduction, based on Galerkin’ projection onto space spanned by empirical modes calculated for direct numerical simulation (DNS) data, is done for flow past a wall-mounted cylinder.

2. Test case description

Circular cylinders are extensively investigated in fluid mechanics [7, 8, 9] due to their importance in fundamental research as well as engineering applications. In the latter case, cylinder-shaped objects are usually finite in length, with one end mounted on a flat wall, for example chimneys, stacks, high-rise buildings and legs of oil platforms [10].

The geometry of wall-mounted cylinders is quite simple, however they are a source of complex, three-dimensional structures in their near wake. In addition to the von Karman vortices known from infinite cylinders, structures like horseshoe vortices (near the wall) and – in the case of finite cylinders – trailing vortices [11] form.

These phenomena lead to the need to consider many important factors, during the design of free-standing structures [12]. These include structural loading associated with velocity and pressure fluctuations [13], heat and mass transfer influenced by high-turbulence mixing zones in the wake (relevant for heat exchangers, heat stacks and wind turbines [14, 15]) and downburst phenomena in the wake, which might transport contamination from chimney stacks or debris from buildings, bringing discomfort and danger to pedestrians [16].

While flows past infinite cylinders are well-studied and many ROM for such flows have been constructed [17, 18], the Galerkin models for the flow past wall-mounted cylinders are much less common [16]. It is expected, that the different behavior of the flow near wall boundary will influence the basis expansion and might be an additional challenge for model order reduction.

In this study, a semi-infinite cylinder mounted on the bottom plane as presented in Fig. 1, is analyzed. The flow domain spans 20 diameters in a streamwise direction, with a rectangular cross-section of size 10×8 diameters. The domain is

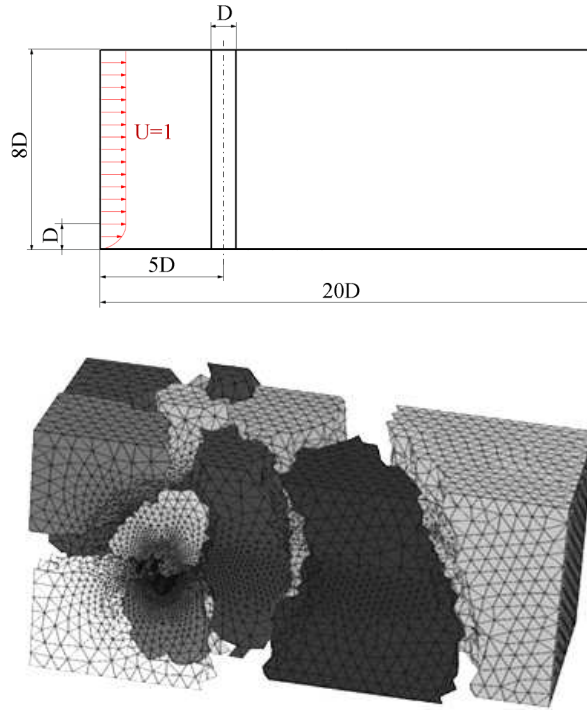


FIG. 1. Computational domain (top) and the mesh partitioned for 16 sub-domains (bottom).

discretized using finite element mesh containing 702 379 second-order tetrahedra elements.

For such configuration, DNS of Navier–Stokes equations was performed using an in-house, parallel solver UNS3 [19, 20], based on the second-order finite element method with Galerkin formulation and quadratic interpolation functions. A penalty formulation with an LBB condition [21] was used to eliminate the pressure from the equations. Nonlinear equations were solved using the iterative Newton–Raphson approach.

The message passing interface (MPI) library provided the communication between the computational nodes and the domain partitioning was done using the Metis package.

Incompressible flow past a wall-mounted cylinder was analyzed for Reynolds number $Re = 400$. Velocity on the inlet, normal to the front surface, was set to $U = U_x = 1$ for all the nodes with a z -coordinate higher than D . Between the bottom wall ($z = 0$) and $z = D$, the parabolic velocity gradient was used. On the side walls and the top of the domain ($z = 8D$), symmetry planes were used.

As an initial solution, steady flow for the same Reynolds number ($Re = 400$) was chosen (Fig. 2, left). For these operating conditions, a steady solution is

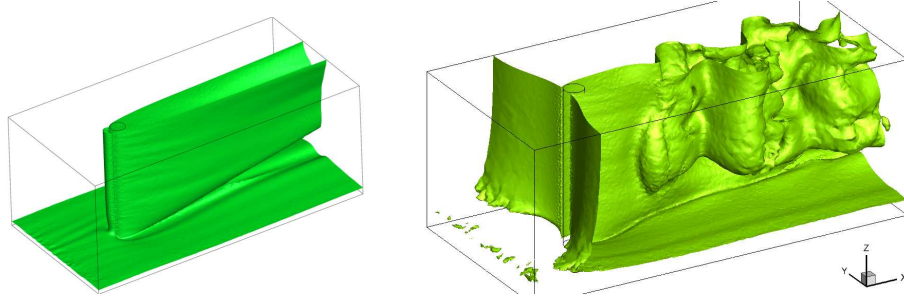


FIG. 2. Flow around a wall-mounted cylinder at $Re = 400$. Velocity isosurfaces for a steady flow (initial solution, left) and an instantaneous solution from fully-developed periodic wake (right).

unstable and difficult to be obtained using a steady solver. Therefore an unsteady solver was used, and the size of the time step was gradually increased. Using this artificial damping, oscillations were suppressed and the flow was stabilized. Finally, the steady solver was used to obtain the fully converged solution.

Next, the unsteady simulation, performed on 16 nodes of a PC-based cluster, resulted in a fully-developed periodic wake, as depicted in Fig. 2 (right).

The cycle interval for the obtained flow is approximately $T = 5.7$ s, which gives predominant vortex shedding frequency $f = 0.175$ Hz.

3. Modal decomposition

The mode bases used in the model reduction can be classified in terms of mathematical, physical and empirical approaches, as discussed in [3]. In the empirical approach, the modes are determined in the decomposition of (previously obtained) experimental or numerical data.

For years, the most popular method of decomposing the spatio-temporal signal was proper orthogonal decomposition (POD) [22] and its variant, called the method of snapshots [23]. The known limitations of these methods, especially in the reconstruction of transitional flow (increasing the amplitude of oscillation) and in further application in reduced order modelling, resulted in intensive research being conducted on decomposition methods. The original idea of POD has been expanded, leading to techniques like bi-orthogonal decomposition (BOD) [24], double POD (DPOD) [25] and balanced POD (BPOD) [26]. On the other hand, the inspection of preexisting methods used in the other areas like principal oscillation patterns (POP) [27, 28] and Koopman analysis of nonlinear dynamical systems [29, 30] has led to the development of techniques like oscillation pattern decomposition (OPD) [31] and dynamic mode decomposition (DMD) [32, 33, 34].

A comprehensive survey of the decomposition methods used in fluid dynamics can be found in [31].

In this paper, dynamic mode decomposition, originally introduced to CFD by SCHMID [33] and ROWLEY [32], is used to compute global modes based on the snapshots of the flow from DNS.

In this method, the time-varying process is approximated by the use of linear operator $\tilde{A} = e^{\Delta t A}$ on the current state vector:

$$(3.1) \quad q(t + \Delta t) \approx e^{\Delta t A} q(t).$$

The right-hand side of the equation above might be approximated by multiplying the sequence of known solutions $V_{0\dots n} = \{q_0, q_1, q_2, \dots, q_n\}$ with the companion matrix \mathbf{S} :

$$(3.2) \quad \tilde{A}V_{0\dots n} \approx V_{0\dots n}\mathbf{S},$$

where

$$(3.3) \quad \mathbf{S} = \begin{pmatrix} 0 & 0 & \dots & 0 & c_0 \\ 1 & 0 & \dots & 0 & c_1 \\ 0 & 1 & \dots & 0 & c_2 \\ \dots & \dots & \dots & \dots & \dots \\ 0 & 0 & \dots & 1 & c_n \end{pmatrix},$$

The coefficients c_0, \dots, c_n of the companion matrix \mathbf{S} are obtained from the solution of the overdetermined system of equations (3.1) (minimizing the norm $\|V_{0\dots n}C - V_{n+1}\|_2$). The eigenvectors of matrix \mathbf{S} are used to obtain the DMD modes, while real and imaginary parts of the eigenvalues determine modal growth rates σ_j and frequencies ω_j :

$$(3.4) \quad \begin{aligned} \sigma_j &= \frac{1}{\Delta t} \operatorname{Re}(\log(\lambda_j)), \\ f_j &= \frac{1}{2\pi\Delta t} \operatorname{Im}(\log(\lambda_j)), \end{aligned}$$

For flow past a wall-mounted cylinder, 171 snapshots from the last three cycles (with sampling frequency $f = 10$ Hz) were used to compute the time-average and DMD modes (Figs. 3–5).

For each complex mode pair, growth rates and frequencies were computed (Fig. 6).

The mode pairs are sorted with respect to the mode norm. The first three mode pairs, after orthonormalization, represent 86% of the turbulent kinetic energy (TKE), and the first six mode pairs represent 98% of TKE.

It can be seen, that the first modes are saturated and the higher modes are more and more damped. Explanation of these decaying growth rates is given

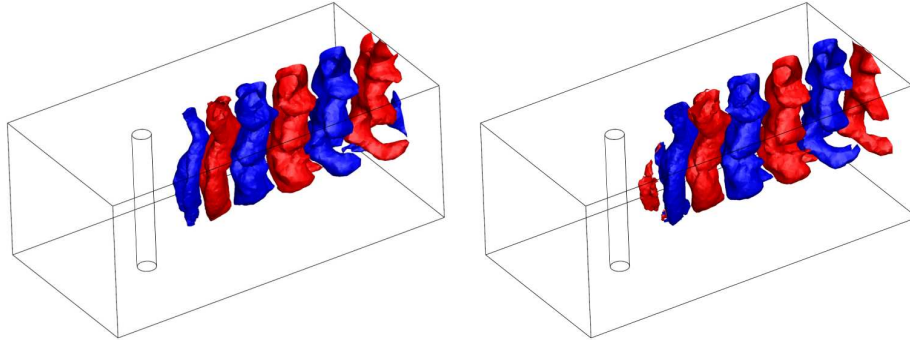


FIG. 3. Isosurfaces of the imaginary (left) and real (right) parts of the first DMD mode pair (frequency $f_1 = 0.176$ Hz, growth rate $r_1 = -0.002$).

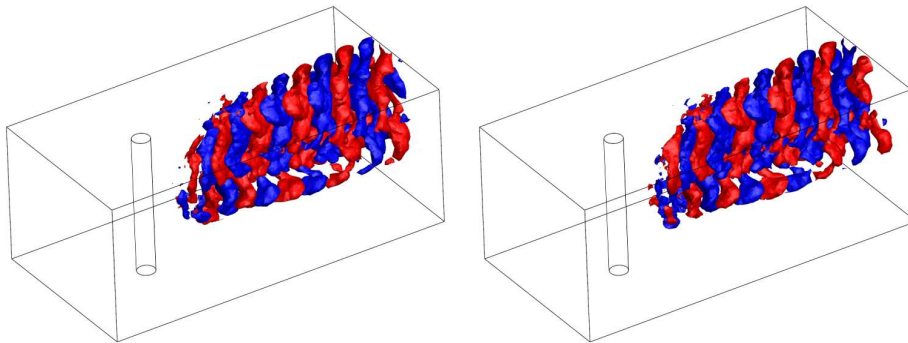


FIG. 4. Isosurfaces of the imaginary (left) and real (right) parts of the second DMD mode pair (frequency $f_2 = 0.352$ Hz, growth rate $r_2 = -0.005$).

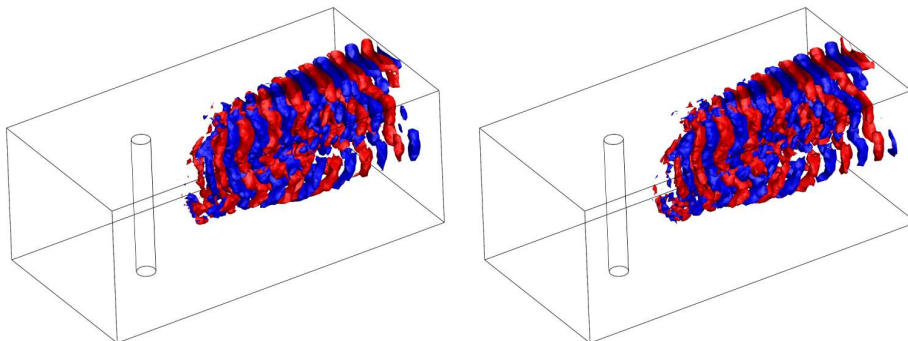


FIG. 5. Isosurfaces of the imaginary (left) and real (right) parts of the third DMD mode pair (frequency $f_3 = 0.527$ Hz, growth rate $r_3 = -0.006$).

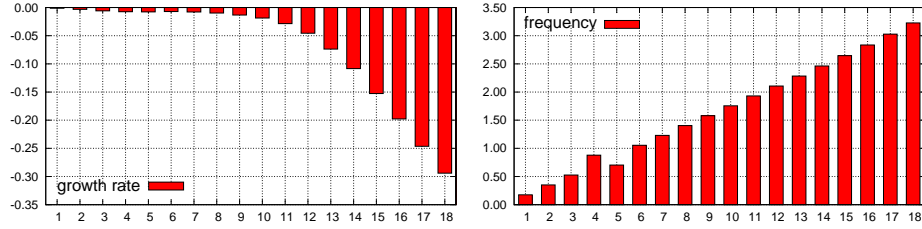


FIG. 6. Growth rates (left) and frequencies (right) for DMD mode pairs.

by BAGHERI [35]: “for any stable limit cycle (...) the remaining eigenvalues $j \neq 0$ are decaying and describe the transient behaviour of flow in the local stable manifold of the limit cycle”.

The frequencies of the further modes are harmonics of the first, fundamental frequency $f_1 = 0.176$ Hz. Mode pairs 4 and 5 are one exception, as they seem to be switched. In a limit cycle, the modes related to the highest frequencies might be neglected [35].

In consideration of the above, the first one mode pair and the first three modes pairs were chosen to build ROMs of the flow.

4. Model reduction using Galerkin projection

One of the methods of reducing the flow model is Galerkin approximation of the variables (e.g., velocities) with base solution \mathbf{u}_0 (steady or time-averaged flow) and a number modes \mathbf{u}_j multiplied by time-dependent mode amplitudes a_j (4.1):

$$(4.1) \quad \mathbf{u}^{[N]} = \mathbf{u}_0 + \sum_{j=1}^N a_j \mathbf{u}_j = \sum_{j=0}^N a_j \mathbf{u}_j, \quad a_0 \equiv 1.$$

In this paper, the mode basis used in the approximation results from the DMD of the snapshots from three cycles of periodic wake flow. Before the modelling, real and imaginary parts of DMD modes were separated and orthonormalized.

The projection of the residual of the approximated Navier–Stokes equation onto the space spanned by the modes (4.2) results in a system of ordinary differential equations, with mode amplitudes as unknowns (4.3).

$$(4.2) \quad (\mathbf{u}_i, R^{[N]})_{\Omega} = \int_{\Omega} \mathbf{u}_i R^{[N]} d\Omega = 0,$$

$$(4.3) \quad \dot{a}_i = \frac{1}{\text{Re}} \sum_{j=0}^N a_j l_{ij} + \sum_{j=0}^N \sum_{k=0}^N a_j a_k q_{ijk},$$

where:

$$(4.4) \quad l_{ij} = (\mathbf{u}_i, \Delta \mathbf{u}_j)_\Omega \quad \text{and} \quad q_{ijk} = -(\mathbf{u}_i, \nabla \cdot (\mathbf{u}_j \otimes \mathbf{u}_k))_\Omega.$$

To achieve the robustness required in flow control applications, low dimensional models of flow past a wall-mounted cylinder were designed using two and six of the most dominant modes from DMD.

The truncation of the mode basis and the possible inconsistency of reduced order formulation and full-dimensional data lead to a loss of quality, which might be improved by using model calibration [36, 37].

Additionally, the truncation of the modal basis to one pair of (the most dominant) modes resulted in instability of the model – the amplitude of oscillation grew to infinity.

To resolve this problem, shift mode \mathbf{u}_Δ [3], also known as zero mode [38], was introduced as a critical enabler for the transient representation of empirical Galerkin models. This additional mode (Fig. 7, right), defined as a normalized mean-field correction, represents the difference between short-term averaged flow and the space spanned by expansion modes (like POD modes) [3]. An overview of shift mode design techniques is given in [39].

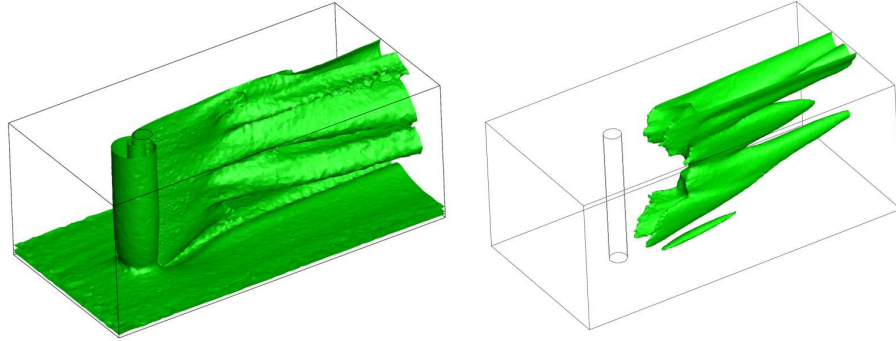


FIG. 7. Isosurfaces of a velocity for time-averaged flow for fully-developed wake (left) and shift mode (right).

Shift mode was orthonormalized with respect to the rest of expansion modes used, i.e.,

$$(4.5) \quad (\mathbf{u}_\Delta, \mathbf{u}_i)_\Omega = 0, \quad i = 1, \dots, N.$$

Galerkin models incorporating shift mode are stable [40] – they have bounded amplitudes of mode coefficients (Fig. 8).

In the case of the model based on two DMD modes (one pair) and shift mode, the amplitude of modes is 1.5 times larger than the one expected for limit-cycle

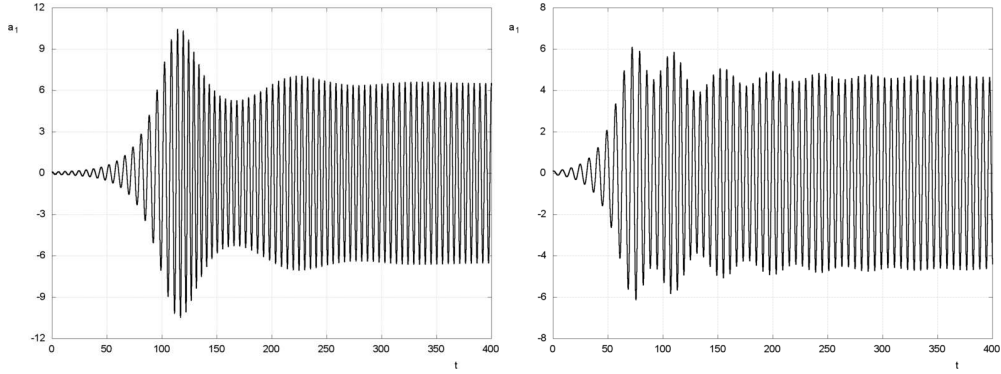


FIG. 8. Fourier coefficients (amplitudes) for the first DMD mode, resulting from Galerkin models based on shift mode and two (left) and six (right) DMD modes.

oscillations. The addition of further four modes improves the model – the amplitudes of the modes (especially the first ones), resulting from the solution of the Galerkin system resemble the ones obtained from the projection of snapshots onto DMD modes (Fig. 9). Unfortunately, the modal frequencies resulting from the reduced model are slightly lower than those obtained from DMD.

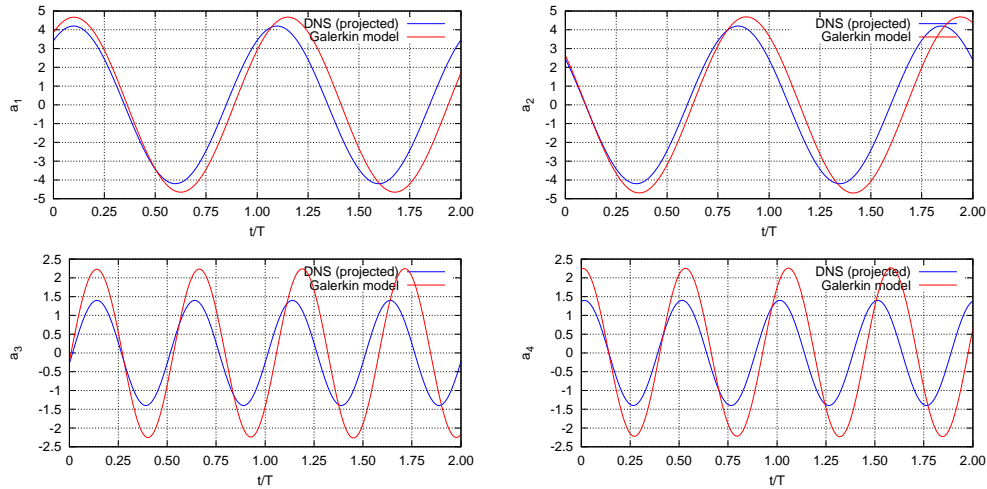


FIG. 9. Fourier coefficients (amplitudes) for the first and third DMD modes used in the Galerkin model, as obtained from the reduced-order Galerkin model and from projection onto snapshots from DNS.

To achieve better agreement in the frequency of vortex shedding and keep the dimension of the model as low as possible, genetic algorithm-based calibration of linear and quadratic terms of the Galerkin system was done, using the approach described in [37]. In this case, objective function F to be minimized was related

to the combined square error of the frequencies f_i and amplitudes a_i of N mode coefficients:

$$(4.6) \quad F = \sum_{i=1}^N \left(\alpha \left(\frac{f_i^{\text{DNS}} - f_i^{\text{ROM}}}{f_i^{\text{DNS}}} \right)^2 + (a_i^{\text{DNS}} - a_i^{\text{ROM}})^2 \right),$$

with the reference modal frequencies f_i^{DNS} and amplitudes a_i^{DNS} (Table 1) obtained from the projection of the DNS-based snapshots onto the space spanned by DMD modes.

Table 1. Reference modal frequencies and amplitudes used in the calibration, as obtained from DNS/DMD.

mode i	frequency f_i^{DNS}	amplitude a_i^{DNS}
1/2	0.176	4.20
3/4	0.352	1.40
5/6	0.528	0.75

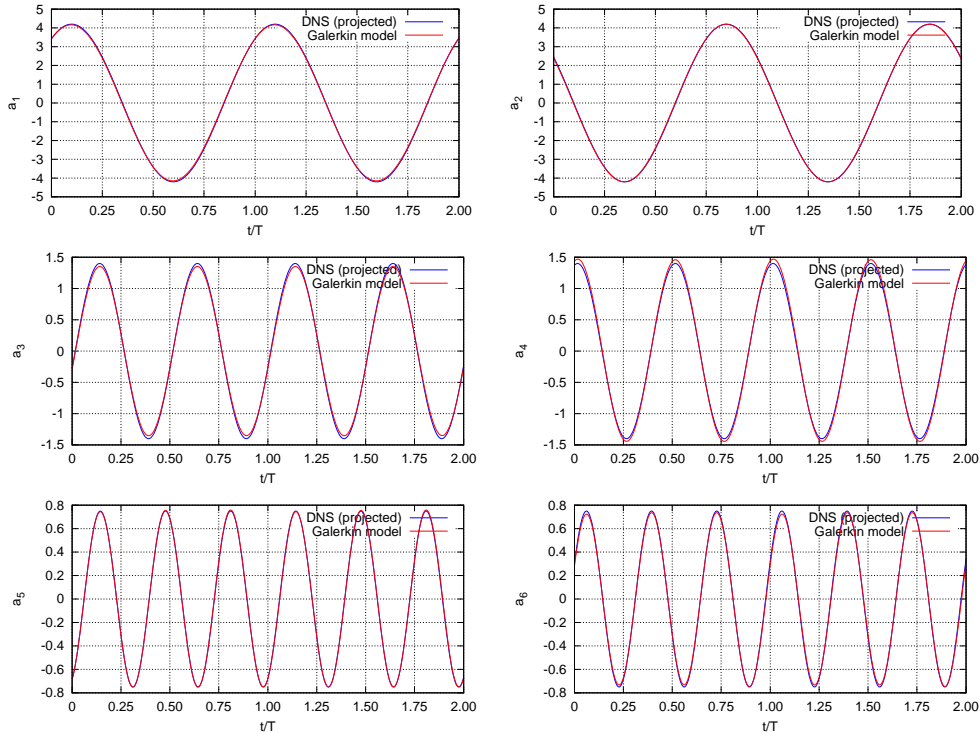


FIG. 10. Fourier coefficients (amplitudes) for six DMD modes used in the Galerkin model, as obtained from the calibrated reduced order Galerkin model and from projection onto snapshots from DNS.

The resulting model accurately captures the level of turbulent kinetic energy K for limit cycle oscillations (Fig. 12). However, the dynamics of the transition from the steady solution could still be improved.

The coefficient $\alpha = 10$ was chosen in order to balance the influence of the frequency and the amplitude differences.

After calibration of the model, the frequencies and amplitudes of mode coefficients (depicted in Fig. 10) agree with the results obtained from DNS and projected onto DMD modes.

The value of the objective function (combined error measure) was reduced almost 400 times, from $F = 3.4695$ to $F = 0.0089$.

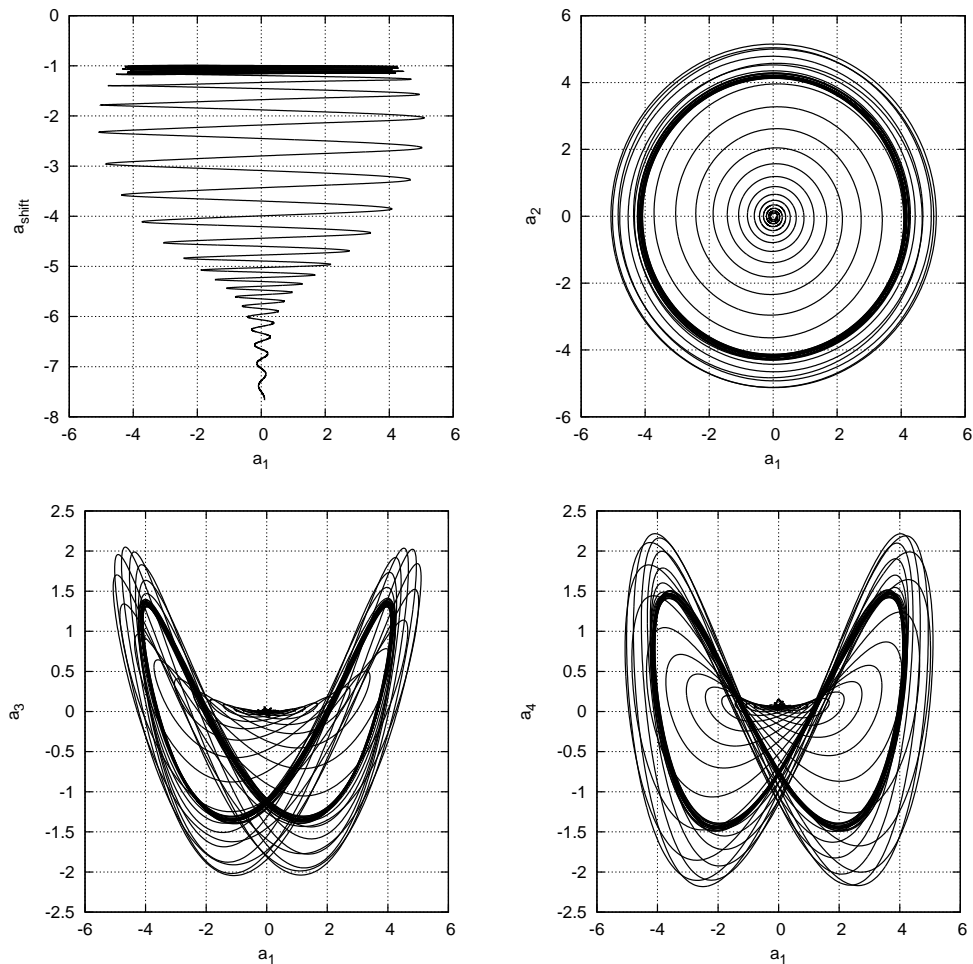


FIG. 11. Generalized phase-average mode behavior; phase portraits for the first four DMD modes and shift-mode (mean field paraboloid, top-left).

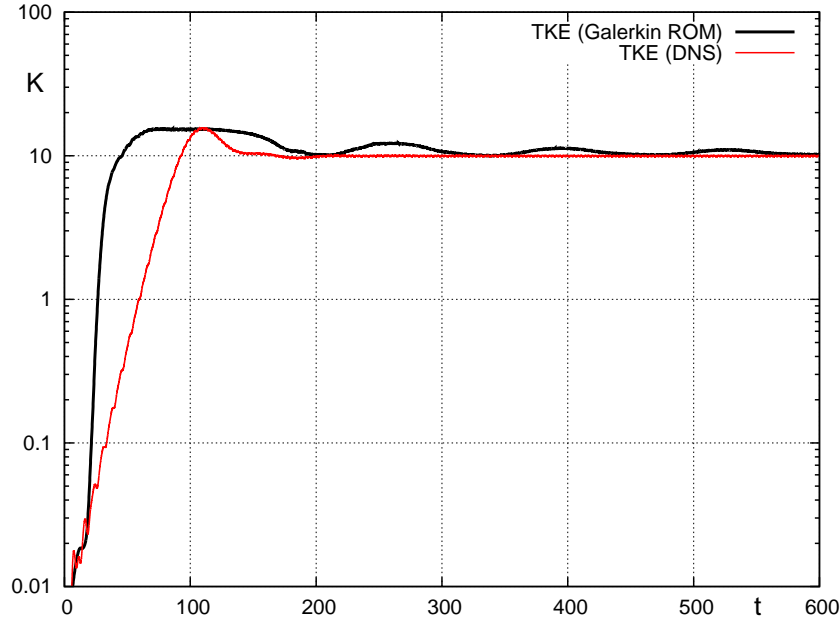


FIG. 12. TKE for the calibrated Galerkin model, compared to DNS.

The obtained low-dimensional (seven-equation) model of flow around the semi-infinite cylinder, mounted to a wall at one end, experienced the dynamics known for flows around cylindrical bodies. Due to this, mean-field theory can be applied. Phase portraits for the mode coefficients (Fig. 11) can be compared with their counterparts from other experiments, for example for flow past a wall-mounted, square cylinder [16].

The model lacks information about the mode shapes in the steady state and their deformation in the transition between the two operating conditions (fixed point and attractor). Accurate modeling of that transition requires the parameterization of mode basis. One of such methods is continuous mode interpolation [41, 42]. This, as well as the long-term, decaying variation of K , will be the subject of further research.

5. Summary

In this paper, a model reduction technique was demonstrated using the example of 3D, viscous flow around a semi-infinite, wall-mounted cylinder at $Re = 400$.

DMD of the snapshots from DNS revealed one fundamental frequency related to the most dominant DMD mode and higher harmonics associated with further modes. The mode basis was truncated and the low-dimensional subspace was spanned on first two and six DMD modes, sorted by mode norm.

The model of the flow was derived using Galerkin projection of the residual of (approximated) Navier–Stokes equations onto space spanned by the most dominant modes. Additionally, the use of shift mode stabilized the model and improved its accuracy.

While the models based on two DMD modes were unacceptable due to large (or even going to infinity) mode amplitudes, Galerkin models based on six DMD modes reproduced the high-dimensional data much better. However, the amplitudes of modes, especially the higher ones, were slightly underestimated.

The Galerkin model based on six DMD modes, with additional calibration based on a genetic algorithm, adequately captured the vortex shedding frequencies for different vortex scales of fully-developed von Karman vortices street. The dynamics of the transition from steady state to fully-developed wake could be improved, by enhancing the model using physical modes representing fixed-point dynamics and, for example, using the technique of continuous interpolation of mode basis [41].

Acknowledgement

This work has been funded by National Centre of Science under research grant no. 2011/01/B/ST8/07264. The authors appreciate the valuable comments provided by the reviewers.

References

1. R. BOURGUET, M. BRAZA, A. SÉVRAIN AND A. BOUHADJI, *Capturing transition features around a wing by reduced-order modeling based on compressible Navier–Stokes equations*, *Physics of Fluids*, **21**, 094104, 2009.
2. J. GERHARD, M. PASTOOR, R. KING, B.R. NOACK, A. DILLMANN, M. MORZYŃSKI, G. TADMOR, *Model-based control of vortex shedding using low-dimensional Galerkin models*, 33rd AIAA Fluids Conference and Exhibit, Paper 2003-4262, 2003.
3. B.R. NOACK, K. AFANASIEV, M. MORZYŃSKI, G. TADMOR, F. THIELE, *A hierarchy of low-dimensional models for the transient and post-transient cylinder wake*, *J. Fluid Mech.*, **497**, 335–363, 2003.
4. W. Stankiewicz, M. Morzyński, R. Roszak, B.R. Noack, G. Tadmor, *Reduced order modelling of a flow around an airfoil with a changing angle of attack*, *Arch. Mech.*, **60**, 6, 509–526, 2008.
5. B.R. NOACK, M. MORZYŃSKI, G. TADMOR (eds.), *Reduced-Order Modelling for Flow Control*, Series: CISM International Centre for Mechanical Sciences, Vol. 528, Springer, 2011.
6. S.L. BRUNTON, B.R. NOACK, *Closed-loop turbulence control: Progress and challenges*, *Applied Mechanics Reviews*, **67**, 5, 050801, 2015.

7. J. FRÖHLICH, W. RODI, *LES of the flow around a circular cylinder of finite height*, International Journal of Heat and Fluid Flow, **25**, 3, 537–548, 2004.
8. CH. DOBRILOFF, W. NITSCHKE, *Surface pressure and wall shear stress measurements on a wall mounted cylinder*, Imaging Measurement Methods for Flow Analysis, 197–206, Springer, 2009.
9. O. FREDERICH, J. SCOUTEN, D.M. LUCHTENBURG, F. THIELE, *Numerical simulation and analysis of the flow around a wall-mounted finite cylinder*, Imaging Measurement Methods for Flow Analysis, 207–216, Springer, 2009.
10. H.F. WANG, Y. ZHOU, J. MI, *Effects of aspect ratio on the drag of a wall-mounted finite-length cylinder in subcritical and critical regimes*, Experiments in fluids, **53**, 2, 423–436, 2012.
11. T. KAWAMURA, M. HIWADA, T. HIBINO, I. MABUCHI, M. KUMADA, *Flow around a finite circular cylinder on a flat plate (cylinder height greater than turbulent boundary layer thickness)*, Bulletin of the JSME, **27**, 232, 2142–2151, 1984.
12. P. SATTARI, J.A. BOURGEOIS, R.J. MARTINUZZI, *On the vortex dynamics in the wake of a finite surface-mounted square cylinder*, Experiments in Fluids, **52**, 5, 1149–1167, 2012.
13. H. SAKAMOTO, S. OIWAKE, *Fluctuating forces on a rectangular prism and a circular cylinder placed vertically in a turbulent boundary layer*, Journal of Fluids Engineering, **106**, 2, 160–166, 1984.
14. T. IGARASHI, *Heat transfer from a square prism to an air stream*, International Journal of Heat and Mass Transfer, **28**, 1, 175–181, 1985.
15. H. WANG, Y. ZHOU, C. CHAN, T. ZHOU, *Momentum and heat transport in a finite-length cylinder wake*, Experiments in Fluids, **46**, 6, 1173–1185, 2009.
16. J.A. BOURGEOIS, B.R. NOACK, R.J. MARTINUZZI, *Generalized phase average with applications to sensor-based flow estimation of the wall-mounted square cylinder wake*, Journal of Fluid Mechanics, **736**, 316–350, 2013.
17. M. GHOMMEM, I. AKHTAR, M.R. HAJJ, I.K. PURI, *A reduced-order model for unsteady flow over circular cylinder*, 8th AIAA Aerospace Sciences Meeting Including the New Horizons Forum and Aerospace Exposition, Orlando, Florida, Paper 2010-1275, 2010.
18. S. ULLMANN, J. LANG, *POD and CVT Galerkin reduced-order modeling of the flow around a cylinder*, Proc. Appl. Math. Mech., **12**, 1, 697–698, 2012.
19. M. MORZYŃSKI, F. THIELE, *3D FEM Global Stability Analysis of viscous flow*, Lecture Notes in Computer Science, Parallel Processing and Applied Mathematics, vol. 4967, 1293–1302, Springer, 2008.
20. M. MORZYŃSKI, F. THIELE, *Finite Element Method for Global Stability Analysis of 3D Flows*, 38th AIAA Fluid Dynamics Conference and Exhibition, Paper 2008-3865, 2008.
21. F. BREZZI, *On existence, uniqueness and approximation of saddle-point problems arising from Lagrange multipliers*, ESAIM: Mathematical Modelling and Numerical Analysis-Modélisation Mathématique et Analyse Numérique, **8**, (R2), 129–151, 1974.
22. G. BERKOOZ, P. HOLMES, J.L. LUMLEY, *The proper orthogonal decomposition in the analysis of turbulent flows*, Ann. Rev. Fluid Mech., **25**, 1, 539–575, 1993.

23. L. SIROVICH, *Turbulence and the dynamics of coherent structures. I-Coherent structures. II-Symmetries and transformations. III-Dynamics and scaling*, Quarterly of Applied Mathematics, **45**, 561–571, 1987.
24. N. AUBRY, R. GUYONNET, R. LIMA, *Spatiotemporal analysis of complex signals: theory and applications*, Journal of Statistical Physics, **64**, 2/3, 683–739, 1991.
25. S. SIEGEL, J. SEIDEL, C. FAGLEY, D.M. LUCHTENBURG, K. COHEN, T. MCLAUGHLIN, *Low-dimensional modelling of a transient cylinder wake using double proper orthogonal decomposition*, J. Fluid Mech., **610**, 1, 1–42, 2008.
26. C.W. ROWLEY, *Model reduction for fluids, using balanced proper orthogonal decomposition*, Int. J. Bifurcat. Chaos, **15**, 3, 997–1013, 2005.
27. K. HASSELMANN, *PIPs and POPs: the reduction of complex dynamical systems using principal interaction and oscillation patterns*, Journal of Geophysical Research, **93**, (D9), 11.015-11.021, 1988.
28. A. GARCIA, C. PENLAND, *Fluctuating hydrodynamics and principal oscillation pattern analysis*, Journal of Statistical Physics, **64**, 5-6, 1121–1132, 1991.
29. A. LASOTA, M.C. MACKEY, *Chaos, fractals and noise: stochastic aspects of dynamics*, Applied Mathematical Sciences, vol. 97, Springer, 1994.
30. I. MEZIĆ, *Spectral properties of dynamical systems, model reduction and decompositions*, Nonlinear Dyn., **41**, 309–325, 2005.
31. V. URUBA, *Decomposition methods in turbulence research*, EPJ Web of Conferences, **25**, 01095, 2012.
32. C.W. ROWLEY, I. MEZIĆ, S. BAGHERI, P. SCHLATTER, D. HENNINGSON, *Spectral analysis of nonlinear flows*, Journal of Fluid Mechanics, **641**, 115–127, 2009.
33. P.J. SCHMID, *Dynamic mode decomposition of numerical and experimental data*, J. Fluid Mech., **656**, 1, 5–28, 2010.
34. O. FREDERICH, D.M. LUCHTENBURG, *Modal analysis of complex turbulent flow*, 7th International Symposium on Turbulence and Shear Flow Phenomena, TSFP-7, 2011.
35. S. BAGHERI, *Koopman-mode decomposition of the cylinder wake*, J. Fluid Mech., **726**, 596–623, 2013.
36. L. CORDIER, B. ABOU EL MAJD, J. FAVIER, *Calibration of POD reduced-order models using Tikhonov regularization*, Int. J. Numer. Meth. Fluids, **63**, 2, 269–296, 2009.
37. W. STANKIEWICZ, R. ROSZAK, M. MORZYŃSKI, *Genetic algorithm-based calibration of reduced order Galerkin models*, Mathematical Modelling and Analysis, **16**, 2, 233–247, 2011.
38. B. PROTAS, J.E. WESFREID, *Drag force in the open-loop control of the cylinder wake in the laminar regime*, Physics of Fluids, **14**, 2, 810–826, 2002.
39. G. TADMOR, J. GONZALEZ, O. LEHMANN, B.R. NOACK, M. MORZYŃSKI, W. STANKIEWICZ, *Shift modes and transient dynamics in low order, design oriented Galerkin models*, 45rd AIAA Aerospace Sciences Meeting and Exhibit, Paper 2007-0111, 2007.
40. M. SCHLEGEL, B.R. NOACK, *On long-term boundedness of Galerkin models*, J. Fluid Mech., **765**, 325–352, 2015.

41. M. MORZYŃSKI, W. STANKIEWICZ, B.R. NOACK, R. KING, F. THIELE, G. TADMOR, *Continuous mode interpolation for control-oriented models of fluid flows*, Active Flow Control, Springer, 260–278, 2007.
42. W. STANKIEWICZ, M. MORZYŃSKI, B.R. NOACK, G. TADMOR, *Reduced order Galerkin models of flow around NACA0012 airfoil*, Mathematical Modelling and Analysis, **13**, 1, 113–122, 2008.

Received September 5, 2015; revised version January 22, 2016.
